

**Local dynamical lattice instabilities: Prerequisites for resonant pairing superconductivity**Julius Ranninger<sup>1</sup> and Alfonso Romano<sup>2</sup><sup>1</sup>*Institut Néel, CNRS-UJF, Boîte Postale 166, 38042 Grenoble, France*<sup>2</sup>*Laboratorio Regionale SuperMat, CNR-INFM, I-84081 Baronissi, Salerno, Italy**and Dipartimento di Fisica “E. R. Caianiello,” Università di Salerno, I-84081 Baronissi, Salerno, Italy*

(Received 7 May 2008; revised manuscript received 17 July 2008; published 27 August 2008)

Fluctuating local diamagnetic pairs of electrons, embedded in a Fermi sea, are candidates for non-phonon-mediated superconductors without the stringent conditions on  $T_c$  which arise in phonon-mediated BCS classical low- $T_c$  superconductors. The local accumulations of charge, from which such diamagnetic fluctuations originate, are irrevocably coupled to local dynamical lattice instabilities and form composite charge-lattice excitations of the system. For a superconducting phase to be realized, such excitations must be itinerant spatially phase-coherent modes. This can be achieved by resonant pair tunneling in and out of polaronic cation-ligand sites. Materials in which superconductivity driven by such local lattice instability can be expected have a  $T_c$  which is controlled by the phase stiffness rather than the amplitude of the diamagnetic pair fluctuations. Above  $T_c$ , a pseudogap phase will be maintained up to  $T^*$ , at which this pairing amplitude disappears. We discuss the characteristic local charge and lattice properties which characterize this pseudogap phase and which form the prerequisites for establishing a phase-coherent macroscopic superconducting state.

DOI: [10.1103/PhysRevB.78.054527](https://doi.org/10.1103/PhysRevB.78.054527)

PACS number(s): 71.38.-k, 74.20.Mn, 72.20.Jv

**I. INTRODUCTION**

Ever since the BCS theory identified the phonon exchange mechanism as the cause for electron pairing leading to a superconducting state and, at the same time, pinned down the order of magnitude of the critical temperature  $T_c$ , considerable efforts have been undertaken to bypass these constraints on  $T_c$ . One of the leading ideas was to look for fluctuating local diamagnetism caused by intrinsic atomic correlations, which would act as an essential component for pairing in the many-body electron wave function. Since diamagnetic pairs of electrons necessarily lead to local lattice deformations, one searched for materials<sup>1</sup> where such deformations would exist on a dynamical level, as close as possible to but not at a global lattice instability. This was thought to favor optimal diamagnetism and strong superconducting correlations, without leading to localization which would originate from static lattice instabilities.

Along this line of thinking, systematic studies were undertaken that searched for compounds liable to show charge disproportionation, originating from unstable “formal” valence states of the cations which build up such structures. Those formal valence states, required by the chemical stoichiometry given a certain crystalline environment, are skipped. As a result, such materials become composed of a mixture of cations, each of which with one more or one less charge. Examples of such valence skippers which are unstable are  $Tl^{2+}$ ,  $Pb^{3+}$ ,  $Sn^{3+}$ ,  $Bi^{4+}$ , and  $Sb^{4+}$ . These elements prefer to exist as  $Tl^{1+}$ ,  $Pb^{2+}$ ,  $Sn^{2+}$ ,  $Bi^{3+}$ , and  $Sb^{3+}$  together with  $Tl^{3+}$ ,  $Pb^{4+}$ ,  $Sn^{4+}$ ,  $Bi^{5+}$ , and  $Sb^{5+}$ . This implies a tendency to electron pairing and for that reason attracted, early on, much attention for possible non-phonon-mediated superconductivity of purely atomic origin. Charge disproportionation then originates from effective negative- $U$  centers, to which the electrons, associated with the cations with unstable valence configurations, are attracted and form bound electron pairs. Casting such physics in terms of a

negative- $U$  Anderson model gives rise to a variety of macroscopic phases, such as charge fluctuation-driven superconductivity,<sup>2-4</sup> correlation-driven insulating states, and translationally symmetry-broken charge-ordered states. For the exactly half-filled band case, the stable valence configurations (differing by two electrons) are degenerate and as a result ensure resonant pair tunneling in and out of charge Kondo impurities.<sup>5</sup>

The mechanism behind valence skipping has been a highly debated subject and for a long time was attributed<sup>6-9</sup> to an intrinsic intra-atomic interplay between the electron affinity and the ionization energy, combined with a crossing of stable closed  $4s$ ,  $5p$ , and  $6s$  electron shells. It has become increasingly evident in recent years that valence skipping and the resulting charge disproportionation systematically appear together with distinct deformations of the cation-ligand complex, which strongly depend on which valence state they are in. Thus, in order to overcome the relatively large on-site Coulomb repulsion,<sup>10</sup> strong Madelung potentials, and strong covalent bonding,<sup>11,12</sup> an adequate polarizability of the material and sufficiently large dielectric constants ( $\approx 20-40$ ) (Ref. 13) must play together so that charge disproportionation can be realized. It is now largely considered that the prime mechanism for charge disproportionation lies in the local lattice relaxations of the ligands surrounding those cations.<sup>14</sup> This picture, closer to the traditional scenario originally hypothesized for localized defects in semiconductors,<sup>15</sup> however now requires taking into account a time retarded—rather than static—exchange interaction between bound electron pairs and itinerant electrons.

The question we address in this paper is to what extent charge disproportionation can be realized in the form of dynamical diamagnetic double-charge fluctuations on effective sites, composed of cations and their surrounding ligand environments. The latter are deformed by local lattice instabilities, which change their bond lengths or angles. In this way, two electrons are either captured from the Fermi sea in the form of a self-trapped bipolaron or released onto the cations

in the immediate vicinity, where they become itinerant again. One can thus hope for a resonant tunneling of pairs of electrons in and out of such polaronic sites, inducing local dynamical pair correlations in the itinerant sector of the electron system. In this sense our scenario is similar to that of fermionic atomic gases, in which a global superfluid phase is induced by a Feshbach resonance<sup>16</sup> which describes the charge-exchange interaction between bound electron-spin triplet states and electron-spin singlet scattering states. For such coherent pair tunneling to occur in our counterpart solid-state example, the charge and ligand deformation fluctuations will have to be highly correlated with each other. We shall examine here to what extent this is feasible. If the exchange of the two types of double-charge carriers is sufficiently efficient, such charge disproportionation materials and, possibly in a wider sense, the copper oxides and their non-BCS-type superconductivity could be due to the resonant bipolaron mechanism described above.

Particularly well studied examples of such materials are:

(a)  $\text{Pb}_{1-x}\text{Tl}_x\text{Te}$ ,<sup>7,8</sup> with the parent compound  $\text{PbTe}$ , which is a small gap semiconductor. Upon doping with Tl, which exists as  $\text{Tl}^{3+}$  in this compound and plays the role of a kind of negative- $U$  center,  $\text{Pb}_{1-x}\text{Tl}_x\text{Te}$  becomes a superconductor with a relatively high value of  $T_c \approx 1.5$  K, considering its small carrier density. For details we refer the reader to an extensive literature on this subject; see Refs. 7 and 8 and references therein.

(b)  $\text{BaBi}_x\text{Pb}_{1-x}\text{O}_3$  (Ref. 17) and  $\text{Ba}_{1-x}\text{K}_x\text{BiO}_3$ , with the parent compound  $\text{BaBiO}_3$ , which is a diamagnetic insulator with a charge-ordered state involving alternating  $\text{Bi}^{\text{III}}$  and  $\text{Bi}^{\text{V}}$ . (From now on we shall use the more appropriate denomination accounting for covalency for the formal valence states, indicated by roman numeral in the superscripts.) Band theory predicts a metal on the basis of a formal valence state  $\text{Bi}^{\text{IV}}$ . The charge-ordered state is stabilized due to a highly anisotropic polarization of the  $O$  ligand environment,<sup>12</sup> inciting positional changes in the two stable valence species of the Bi ions.  $\text{Bi}^{\text{V}}$  is in a regular octahedral ligand environment, with a Bi-O distance of 2.12 Å.  $\text{Bi}^{\text{III}}$  is in a pseudo-octahedral ligand environment where one of the six oxygen ions in the octahedra is displaced to such an extent (with a corresponding Bi-O distance of 2.28 Å) that it is effectively becoming  $\text{O}^{2-}$  after having transferred an electron to the cation.<sup>18</sup> The total outcome is a structurally different ligand environment which favors a  $\text{Bi}^{\text{III}}$  valence state. Partially substituting Ba by K results in a superconducting state with a relatively high value of  $T_c \approx 30$  K, which has been considered as an example of superconductivity induced by double-valence fluctuations.<sup>2-4</sup>

(c) Charge disproportionation is also seen on a molecular, rather than atomic, level in systems such as  $\text{Ti}_4\text{O}_7$ ,<sup>19</sup>  $\text{V}_2\text{O}_5$ ,<sup>20</sup> and  $\text{WO}_{3-x}$ ,<sup>21</sup> in which one observes diatomic pairs of  $\text{Ti}^{\text{III}}\text{-Ti}^{\text{III}}$  together with  $\text{Ti}^{4+}\text{-Ti}^{4+}$ ,  $\text{V}^{\text{IV}}\text{-V}^{\text{IV}}$  together with  $\text{V}^{\text{V}}\text{-V}^{\text{V}}$ , and  $\text{W}^{\text{V}}\text{-W}^{\text{V}}$  together with  $\text{W}^{\text{VI}}\text{-W}^{\text{VI}}$ . These different valence states of the molecular units again show distinctly different intramolecular distances, such as 2.8 Å for  $\text{Ti}^{\text{III}}\text{-Ti}^{\text{III}}$  and 3.08 Å for  $\text{Ti}^{\text{IV}}\text{-Ti}^{\text{IV}}$  bonds. Moreover, with increasing temperature these systems exhibit a thermally activated conductivity by pair hopping. This demonstrates the stability of such bound electron pairs on deformed molecular

units which are locked together in a dynamical fashion with the charge fluctuations.

(d) Indications of dynamical charge fluctuations are also seen in the cuprate superconductors. Here the situation is however more involved. Stable valence states of Cu exist as:

(i)  $\text{Cu}^{\text{I}}$  in a dumbbell oxygen ligand environment, with a characteristic Cu-O bond length of 1.84 Å (examples are  $\text{Cu}_2\text{O}$ ,  $\text{BaCu}_2\text{O}_2$ , and  $\text{FeCuO}_2$ );

(ii)  $\text{Cu}^{\text{II}}$  in square planar oxygen ligand environments, with a characteristic Cu-O bond length of 1.94 Å (an example is  $\text{CuO}_4$ ); and

(iii)  $\text{Cu}^{\text{III}}$  in square planar oxygen ligand environments, in rare cases, with a characteristic Cu-O bond length of around 1.84 Å and hence practically identical to that of  $\text{Cu}^{\text{I}}$  in dumbbell environments<sup>18</sup> (an example is  $\text{KCuO}_2$ ).

In the cuprates the formal valency of Cu lies between II and III. The square lattice of the cuprates is neither a strict square planar nor a dumbbell ligand environment and there is no indication of a static disproportionation of  $\text{Cu}^{\text{II}}$ .  $\text{Cu}^{\text{III}}$ , which should be favored in this cuprate planar lattice structure, could appear only through rapid metallic fluctuations or be due to the stoichiometry of the structure, with an atypical Madelung potential.<sup>22</sup> Yet, local dynamical lattice fluctuations involving the oxygen ligands of the planar Cu ions, the Cu-O bond-stretch (or buckling) modes, exist. They can be considered as being linked to charge fluctuations involving local ligand environments which are typical of stable  $\text{Cu}^{\text{I}}$  and  $\text{Cu}^{\text{III}}$ . In the antinodal region of the Brillouin zone, where the electronic density of states (DOS) is dominated by the pseudogap phenomenon, local scanning tunneling microscope (STM) spectroscopy<sup>23</sup> did establish a strong coupling of electrons with wave vectors  $[k_x, k_y] = [\pm\pi, 0]$  and  $[0, \pm\pi]$  and local phonon modes with characteristic frequencies distributed around 50 meV. The isotope variation of these modes (most likely associated with the Cu-O bond-stretch mode) correlates with that of the pairing gap. This strongly indicates that this local Cu-O bond-stretch mode could play a significant role in the pairing mechanism of the cuprates.

If double-charge fluctuations do play a significant role in establishing a superconducting phase, they have to sustain a free-particle-like behavior with spatial phase coherence. This should occur in spite of the sizable lattice relaxation which, *a priori*, tends to render them rather diffusive. If in this largely diffusive dynamics we can obtain a finite component of coherent phase-correlated double-charge fluctuations, then a superconducting state can materialize. Such a state does not describe a purely bosonic system of bipolarons and bipolaronic superconductivity but is characterized by resonating bipolarons embedded in a Fermi sea. Their signature is a pseudogap in the single-particle DOS at the Fermi level due to strong pairing correlations above the superconducting phase. This scenario has been discussed in great detail over the past years on the basis of the boson-fermion model by Ranninger and collaborators.

To address the question of the feasibility of coherent pair tunneling, we consider charge carriers capable of existing either as self-trapped bipolarons or as itinerant quasifree tight-binding charge carriers on small clusters consisting of the following:

(i) Cation-ligand complexes which are deformable and which can capture the charge carriers in form of bipolarons.

(ii) Square plaquettes composed of four structurally identical cation-ligand complexes (surrounding the deformable central cation-ligand complex), which we consider as undeformable. Charge carriers on these plaquettes shall hence move as itinerant entities rather than be captured by polaronic effects.

Double-charge fluctuations in the present picture imply fluctuations between doubly occupied and unoccupied sites, driven by charge carriers tunneling in and out of such sites and ultimately resulting in pair correlations among those on the plaquette sites. Such essentially local physics contains the essence of triggering a crossover from an insulating purely charge-disproportionated state to a superconducting state upon tuning certain parameters such as the electron-lattice coupling, the adiabaticity ratio, and the charge-carrier density. This physics, intrinsically related to a very local mechanism,<sup>24</sup> manifests itself in the single-particle spectral function, the local diamagnetism, the local phonon softening, the quasielastic peak in the neutron-scattering cross section for the phonons, and the double-peaked pair distribution function for the bond-length fluctuations.

In Sec. II we discuss the salient features of such double-charge fluctuations driven by bond-length fluctuations and present a scenario in terms of a kind of Holstein model which takes into account the different ligand fluctuations characterizing the various charge configurations. In Sec. III we propose a model Hamiltonian which we consider to be adequate for describing the local physics of such systems. We discuss its basic features as far as the efficiency of local pair tunneling is concerned and how such dynamically correlated charge-ligand deformation fluctuations are locked together in order to form phase-coherent correlated itinerant excitations on a short spatial scale. In Sec. IV we discuss the specific characteristics of: (i) the local lattice dynamics close to instabilities, phonon softening, the quasielastic peak in the dynamical structure factor, and the double-peak-structured pair distribution function; and (ii) the diamagnetic correlations induced among the itinerant electrons via such dynamical local lattice instabilities and how they manifest themselves in a pseudogap feature in the electronic density of states. In Sec. V, we briefly review the main findings of the present work and discuss the further issues which have to be treated next.

## II. ELECTRON LOCALIZATION VERSUS DELOCALIZATION IN ELECTRON-LATTICE COUPLED SYSTEMS

The crossover from metallic or superconducting behavior to localized behavior in electron-lattice coupled systems has been a topic of long-standing interest and debate.<sup>25</sup> The issue has been reinvestigated with renewed vigor in recent years, when it became apparent that an insulating phase of localized polaronic charge carriers, bordering on a superfluid phase, can be induced by many-body correlation effects.<sup>26–28</sup> Earlier widely pursued ideas considered density-driven stripping off of the phonon clouds of individual polarons<sup>29,30</sup> and related to it a possible breakdown of Wigner polaron crystallization<sup>31,32</sup> into a metallic phase. Correlation-driven

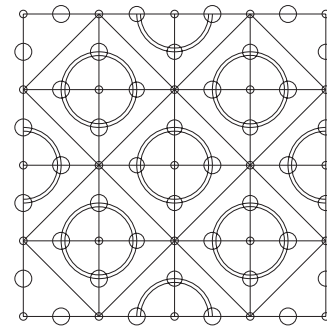


FIG. 1. Paradigm of a two-dimensional (2D) resonant pairing system in terms of a bipartite lattice composed of polaronic cation-ligand complexes (rings) comprising four anions (large circles) in the center of interlinked plaquettes of four metallic cation sites (small circles) housing the charge carriers in itinerant states.

localization can be turned into correlation-driven superconductivity by small modification of certain tunable experimental parameters. Real systems where such and similar phase changes are manifest (cuprates, manganites, transition-metal oxides, and magnesium diborides, just to name a few) are complex in their structure as well as in the composition of their metal-ion-ligand electronic configurations. Their particularity lies in the prevailing local physics, which has been generally overlooked in theoretical studies of the polaron problem. This local physics nevertheless dictates the outcome of macroscopic states such as: (i) a superconducting phase of itinerant electrons with Cooper pairing, (ii) an insulating phase of localized bipolarons, and, possibly, (iii) a phase corresponding to a Bose metal sandwiched between the two, which has become of particular interest in recent years.<sup>33–35</sup> Since the physics of electron-lattice coupled systems involves local atomic or molecular displacements, it requires a description in terms of small polarons, i.e., electrons dragging with them a sizable local lattice deformation which can be on the order of a tenth or so of the lattice constant. We have for that reason to rely on the picture of a Holstein-type molecular crystal model as the basis of our study.

As a paradigm for systems with resonant pairing induced by local lattice deformations, we can imagine as the simplest scenario a bipartite lattice such as the one illustrated in Fig. 1 and consisting of:

(a) a sublattice of polaronic sites, where the charge carriers couple locally and strongly to the molecular deformations of the ligands, resulting in localized bipolaronic bound pairs in the cation-ligand bonds; and

(b) a sublattice of nonpolaronic sites on which the electrons (holes) move as itinerant charge carriers.

When the charge transfer between the two sublattices is switched on, the electron (hole) pairing on polaronic sites, leading to localized bipolarons, will compete energetically with the itinerancy of uncorrelated charge carriers on the nonpolaronic sites in their immediate vicinity, when their respective energies are comparable. This induces pair correlations among the otherwise intrinsically uncorrelated itinerant charge carriers in locally very *confined* regions of the lattice. On a macroscopic scale, this local physics (when

treated on the basis of a heuristic boson-fermion model scenario) ultimately results in a competition between a correlation-driven insulating phase and a superconducting one.<sup>35,36</sup> The transition from one phase into the other can be tuned by varying the strength of the electron-lattice coupling, the size of the adiabaticity ratio, the relative ionic potential difference between the polaronic and the nonpolaronic sites, and the concentration of the charge carriers. Specific interconnected local properties in such systems, which are determinant for the physics on a macroscopic scale, are:

(i) the generation of an intrinsic pseudogap feature in the local electronic density of states,<sup>34,35</sup> which, depending on the parameters of the system, foreshadows an insulating or a superconducting gap;

(ii) the strong softening and a concomitant increase in the spectral weight of local vibrational modes on the polaronic sites,<sup>24</sup> serving as a basic ingredient for the bipolarons to acquire itinerancy and assuring a component of bosonic charge-carrier transport; and

(iii) the double-peak structure in the local lattice displacement pair distribution function due to a quantum coherent superposition<sup>24</sup> of bipolarons and pairs of intrinsically uncorrelated electrons in their immediate vicinity, which can result in dynamically fluctuating stripe-type topological structures.

The approach to the polaron problem followed here is similar to procedures followed in the correlation problem,<sup>37</sup> based on Anderson's resonating valence bond (RVB) idea.<sup>38</sup> There, an intrinsic underlying magnetic structure leads to the formation of local singlet hole pairs on plaquettes, dynamically exchanging with pairs of uncorrelated itinerant holes in their immediate vicinity. As concerns the connections to other electron-phonon models, the present paradigm of a fluctuating bipartite lattice structure of polaronic and nonpolaronic effective sites is qualitatively different from the usually studied molecular crystal Holstein model, where all the sites are considered to be equivalent. Moreover, when the attention is focused on charge Kondo-type resonance features,<sup>39–41</sup> the local electron-phonon coupling is assumed to be of the form  $\hbar\omega_0\alpha(n_{i,\uparrow}+n_{i,\downarrow}-1)[a_i^++a_i]$ ; i.e., it is at any site symmetric with respect to the single-site occupation. On the other hand, as we have stressed in the beginning, systems with double-charge fluctuations show strong anisotropy of their ligand deformations. This motivates us to take an asymmetric electron-lattice coupling of the form  $\hbar\omega_0\alpha(n_{i,\uparrow}+n_{i,\downarrow})[a_i^++a_i]$ . Although the modulus of the displacements of either unoccupied or doubly occupied sites relative to the singly occupied sites, i.e.,  $\langle a_i^++a_i \rangle = \pm 2\alpha(n_{i,\uparrow}+n_{i,\downarrow})$ , is the same for the two types of couplings (symmetric and asymmetric), the respective energies, related to the electron-lattice coupling, are not. For the usual symmetric electron-phonon coupling, the energies of the unoccupied and doubly occupied site are degenerate. It is this which results in the Kondo-type resonance in the charge channel<sup>39–41</sup> provided that the chemical potential of the system is such that this degeneracy, representing the two stable valence configurations, is guaranteed, which is the case for the exactly half-filled band limit. Away from this limit, this is not the case and the resonance disappears.<sup>41</sup> A further and essential difference between the generic Holstein scenario and the present paradigm for resonant pairing systems is that in the valence fluctuation sce-

nario the ligands of two adjacent cations have an anion in common. This leads to strong intersite correlations between cations with different valence states and correspondingly different ligand environments compatible with this bridging oxygen. These facts differentiate between sites where the bipolarons form and sites in the immediate vicinity where they do not. This is similar to what happens with Zhang-Rice singlets in cuprates,<sup>42,43</sup> where singlet pairs form on a Cu ion and its immediate ligand environment of four oxygens but where nearest-neighboring Cu ions cannot behave as such Zhang-Rice singlets at the same time. This "exclusion" feature<sup>44</sup> introduces in the end strong local correlation effects in the band structure of the whole system, which is part of the salient features of the cuprates. Our proposition here is that the local polaronic features of double-charge fluctuations should have a similar effect on the overall band structure and in particular will give rise to a charge pseudogap of polaronic origin.

### III. MODEL

The aim of this work is to examine the local physics of polaronic systems lending themselves to double-charge fluctuations, coupled via an exchange term to itinerant charge carriers. They impose on the latter strong local dynamical diamagnetic fluctuations, which can eventually lead to a global phase-locked superconducting state. We shall do this here, having in mind the cuprates and in particular their normal phase properties. These systems are more complicated than the paradigm for resonant pairing systems discussed in Sec. II, in the sense that all the Cu cations are intrinsically equivalent and there is no translational symmetry breaking to be expected from the outset. Yet we had early-on strong experimental indications<sup>45</sup> that the structural correlations and deformations in the cuprates show remnant bipartite lattice features, on a local level as well as on a finite time scale. These topologically different features, generally referred to as "stripes," break the translational, as well as the rotational, symmetry on a local level.

The application of the valence fluctuation scenario, describing possible resonant pairing in high- $T_c$  superconducting cuprates, implies, for the reasons clarified below, the consideration of three formal valence configurations in the  $\text{CuO}_2$  layers,  $\text{Cu}^{\text{I}}$ ,  $\text{Cu}^{\text{II}}$ , and  $\text{Cu}^{\text{III}}$ . Distinct ligand deformations are associated with them, dumbbell for  $\text{Cu}^{\text{I}}$  and square planar for  $\text{Cu}^{\text{II}}$  and  $\text{Cu}^{\text{III}}$ , but differing from each other in the value of the Cu-O distances (see Fig. 2). The Cu cations in the  $\text{CuO}_2$  layers of the insulating parent compound have a square oxygen ligand environment with Cu-O distances equal to 1.94 Å and are in formal valence state  $\text{Cu}^{\text{II}}$ , according to their chemical composition. Moreover, the cuprates represent a metastable structure characterized by a geometric misfit of the various layers,<sup>46</sup> which leads to Cu-Cu distances in the  $\text{CuO}_2$  layers which can accommodate such  $[\text{Cu}^{\text{II}}\text{-O}_4]$  units [see Fig. 2(a)] only by pushing the oxygens alternately slightly above and below these layers. This structural effect is usually called buckling.

Upon hole doping one introduces single holes in such  $[\text{Cu}^{\text{II}}\text{-O}_4]$  units, which make them turn into  $[\text{Cu}^{\text{III}}\text{-O}_4]$  units,

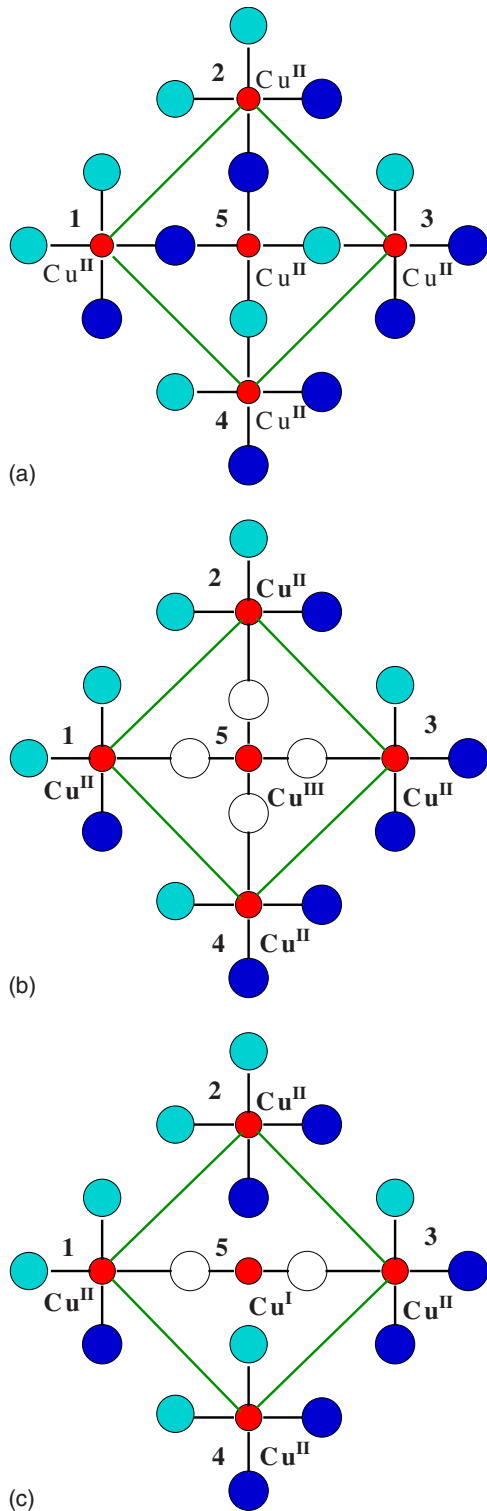


FIG. 2. (Color online) Basic cluster in double-valence fluctuation-driven pairing on the  $\text{CuO}_2$  planes consisting a central Cu cation oxygen ligand environment in three different formal valence states,  $\text{Cu}^{\text{II}}$ ,  $\text{Cu}^{\text{III}}$  and  $\text{Cu}^{\text{I}}$ , illustrated in (a), (b), and (c), respectively. Such central cation-ligand units are linked via a common bridging oxygen to neighboring  $\text{Cu}^{\text{II}}\text{-O}_4$  units. The small red circles denote the Cu cations and the large circles the oxygens. Dark blue means that they are pushed above the  $\text{CuO}_2$  planes, light blue that they are below, and white circles that they are in plane.

with shortened Cu-O distances equal to 1.84 Å. Referring to our small cluster, such a doped effective cation-ligand unit is represented by the central effective site 5 in Fig. 2(b). The reduction to 1.84 Å of the bond lengths in the  $[\text{Cu}^{\text{III}}\text{-O}_4]$  units is accompanied by an unbuckling of the four oxygen cations belonging to these units, which are pulled into the  $\text{CuO}_2$  plane but keep unaltered their distances from the  $\text{Cu}^{\text{II}}$  ions on the plaquette sites, thus inducing no long-range stress field. In this way, the oxygen cations surrounding each of the  $\text{Cu}^{\text{II}}$  ions [located at sites 1–4 in Fig. 2(b)] are still all at the same distance of 1.94 Å from it, but one of them [the bridging oxygen between  $\text{Cu}_5$  and  $\text{Cu}_i$  ( $i=1-4$ )] now lies on the  $\text{CuO}_2$  plane and not above or below it.

We conjecture that the  $[\text{Cu}^{\text{III}}\text{-O}_4]$  units with their doping-induced ligand deformations act as polaronic traps, binding two holes in the form of a localized bipolaron. If the energy of this state is almost degenerate with that of the hole states at the Fermi level, then this bipolaron can split into two holes going on the surrounding matrix. As a consequence,  $[\text{Cu}^{\text{III}}\text{-O}_4]$  turns into  $[\text{Cu}^{\text{I}}\text{-O}_4]$ . As pointed out in Sec. II,  $\text{Cu}^{\text{I}}$  is typically in a linear O-Cu-O dumbbell configuration. If we suppose that this happens also in the  $\text{CuO}_2$  layers, we are faced with two degenerate O-Cu-O dumbbell bonds along the  $x$  and  $y$  directions, with a shortened bond length of 1.84 Å [see Fig. 2(c)], which is the same as for the  $[\text{Cu}^{\text{III}}\text{-O}_4]$  units. This would cause an anisotropic unbuckling of the corresponding bridging oxygens in either one or the other direction but leaving the  $\text{Cu}^{\text{II}}\text{-O}_4$  units on the plaquette sites unaltered, as far as their Cu-O bond lengths are concerned. It is also feasible that, given this directional degeneracy of the bonds of the  $\text{Cu}^{\text{I}}$  valence states, an isotropic ligand deformation with the same bond length of 1.84 Å materializes, due to  $d_{x^2-y^2}$  hybridization in the  $\text{CuO}_2$  plane<sup>47</sup> and which then would be very similar to the configuration illustrated for the  $\text{Cu}^{\text{III}}\text{-O}_4$  unit in Fig. 2(b). It would lead to an isotropic unbuckling, again with no changes in the bond lengths of the cation-ligand units on the plaquettes.

The microscopic foundation of the various formal valence configurations, conjectured here to play a role in the cuprates, is left to be investigated in the future. For the present study, where we shall treat the ligands as an effective deformable scalar quantity, we do not deal with such detailed questions concerning the anisotropy of the deformations on the central sites acting as resonating bipolaronic traps. The valence fluctuations involving the central  $[\text{Cu}^{\text{III}}\text{-O}_4]_5$  unit lead to the release of two holes from the latter onto the neighboring  $[\text{Cu}^{\text{II}}\text{-O}_4]_i$  units on the plaquette sites  $i=1-4$ , and vice versa ( $[\text{Cu}^{\text{III}}\text{-O}_4]_5 \Leftrightarrow [\text{Cu}^{\text{I}}\text{-O}_4]_5 + \text{two holes}$ ). Once on the plaquette units, these holes engage in itinerant states which prevent them from getting localized in form of self-trapped bipolarons on those  $[\text{Cu}^{\text{II}}\text{-O}_4]_i$  units. Such a mechanism describes tunneling in and out of hole pairs from a given central deformable ligand  $[\text{Cu}\text{-O}_4]_5$  unit (our effective site 5) into the surrounding  $[\text{Cu}^{\text{II}}\text{-O}_4]_i$  units which remain essentially undeformed. For this reason we neglect here any charge-ligand deformation coupling on those plaquette sites.

We remind the reader that formal valence in such systems has to be interpreted in terms of the charges involved in the covalent bonds between the cations and their ligand environments and not simply in terms of the charges on the cation.

In the cuprates the covalent character in the  $\text{CuO}_2$  planes is very pronounced. This might be one reason why spectroscopically neither  $\text{Cu}^{\text{III}}$  nor  $\text{Cu}^{\text{I}}$  has been detected so far. Furthermore, given the fact that the three formal valence states  $\text{Cu}^{\text{I}}$ ,  $\text{Cu}^{\text{II}}$ , and  $\text{Cu}^{\text{III}}$  have different ligand environments, the coupling of those deformations to the charge will in general not be symmetric with respect to singly occupied units  $[\text{Cu}^{\text{II}}\text{-O}_4]$ . In the planar  $\text{CuO}_2$  layer of the cuprates, all the Cu ions are equivalent and their charge coupling to the ligand deformations are spatially homogeneous. But this coupling does depend on the formal Cu valence state which is active at any given moment. If we consider the cuprates as being made out of an ensemble of overlapping clusters, as given in Fig. 2, this immediately leads to local dynamical correlations between neighboring ligand deformations. On a short range we can therefore expect that this will naturally lead to intercalated topological local structures. The anisotropy of the O-Cu-O bonds could be relevant for the anisotropic local symmetry breaking.

The construction of a macroscopic state on an infinite lattice, starting from a spatially translationally invariant Hamiltonian but working in a representation of such finite cluster states, which contain the essential local physics, can in principle be achieved. One way would be using renormalization-group techniques such as the plaquette contractor method, based on small clusters of the form illustrated in Fig. 2. This method was developed by Morningstar and Weinstein<sup>48</sup> and applied to the RVB scenario by Altman and Auerbach.<sup>37</sup> For the present scenario of valence fluctuation-driven pairing, including the various ligand deformations correlated with the formal valence state of the clusters presents a formidable numerical task. Questions like that will be addressed in some future work.

Here we shall content ourselves with studying the dynamics of such basic clusters making up the  $\text{CuO}_2$  layers, which permits us to draw some preliminary conclusions on such macroscopic phases. Considering an ensemble of such spatially and temporarily uncorrelated fluctuating clusters, without any long-range spatial phase coherence between them, allows us to describe certain features of the pseudogap phase in the cuprates and its corresponding onset temperature  $T^*$ . We can assess the frequency of the resonant pair tunneling processes, driven by the local ligand deformation fluctuations (which play the role of local dynamical lattice instabilities in a macroscopic system) and which can be approximately related to the mass of the diamagnetic pair fluctuations and thus to the value of  $T_c$  for the onset of a Bose-Einstein condensation-driven superconductivity.

In order to capture the salient features of the local physics of valence fluctuations in the cuprates, as exposed above, we illustrate in Figs. 2(a)–2(c) the various valence configurations of such clusters, where the central Cu cation is alternatively in a  $\text{Cu}^{\text{I}}$ ,  $\text{Cu}^{\text{II}}$ , and  $\text{Cu}^{\text{III}}$  formal valence state. We address this local problem here in a somewhat simplified version, neglecting the detailed structure of the oxygen ligand environments surrounding the Cu cations. For that purpose we assume the  $[\text{Cu-O}_4]_5$  unit to be composed of: (i) a central cation surrounded by an isotropically deformable ligand environment of four anions on an effective site 5 and (ii) four neighboring  $[\text{Cu-O}_4]_i$  units ( $i=1-4$ ) on the

plaquette, representing nonpolaronic sites for which we consider the charge-ligand deformation coupling to be inactive. This is because we consider the charge carriers on the plaquette sites to move as itinerant entities and those ligands have no time to respond to the charge-deformation coupling. They remain in their buckled configurations, corresponding to the  $[\text{Cu}^{\text{II}}\text{-O}_4]_i$  units. We shall denote the hopping rate between the plaquette sites by  $t$  and that between the latter and the central polaronic deformable unit by  $t^*$ . The dimensionless coupling between the charge density and the local ligand deformations is denoted by  $\alpha$  and the bare vibrational frequency of the bond-length fluctuations of that latter by  $\omega_0$ . We assume that the ionic levels of the plaquette sites and of the polaronic sites have a difference in energy, given by  $\Delta$ . The reason for that is the following: Our picture is that the local clusters, as illustrated in Fig. 2, represent the essential dynamical units of the cuprate  $\text{CuO}_2$  planes. In this picture, the states of holes on the plaquette sites play the role of the states of itinerant holes in an infinite system close to the Fermi level, moving in a Hubbard-correlated fashion. The holes we tackle are those induced by doping the parent compound of the correlated problem but which, on an individual cluster, we shall simply treat as itinerant uncorrelated holes on the plaquette. Including the Hubbard  $U$  in this problem would require one to consider at the same time the electronic correlations on the polaronic sites, leading to Zhang-Rice singlets, and those on the plaquette sites, reflecting their pairing in the overall density of states near the Fermi level. This is, however, beyond the present description.

Given these considerations, the Hamiltonian describing such cluster is

$$\begin{aligned}
 H = & -t \sum_{i \neq j=1, \dots, 4, \sigma} [c_{i, \sigma}^\dagger c_{j, \sigma} + \text{H.c.}] - t^* \sum_{i=1, \dots, 4, \sigma} [c_{i, \sigma}^\dagger c_{5, \sigma} + \text{H.c.}] \\
 & + \Delta \sum_{\sigma} c_{5, \sigma}^\dagger c_{5, \sigma} + \hbar \omega_0 \left[ a^\dagger a + \frac{1}{2} \right] \\
 & - \hbar \omega_0 \alpha \sum_{\sigma} c_{5, \sigma}^\dagger c_{5, \sigma} [a + a^\dagger], \quad (1)
 \end{aligned}$$

where  $c_{i\sigma}^{(\dagger)}$  denote the annihilation (creation) operator for a hole with spin  $\sigma$  on site  $i$  and  $a_5^{(\dagger)}$  denote the phonon annihilation (creation) operator associated with the deformable cation-ligand complex at site 5. This local Hamiltonian describes a competition between localized bipolaron hole pairs on the central cation-ligand complex and itinerant holes on the plaquette sites, when the energies of the two configurations are comparable, i.e., for  $2\Delta - 4\hbar\omega_0\alpha^2 \simeq -4t$ . We illustrate in Fig. 3 the variation with  $\alpha$  of the low-energy spectrum of such a system for a set of parameters ( $t=0.2$ ,  $t^*=0.15$ ,  $\Delta=0.5$ , and  $\omega_0=0.1$ , in bare units) corresponding to a typical region in the parameter space  $[\omega_0/t, \hbar\omega_0\alpha^2/t]$  where resonant pairing is well pronounced and rather robust against thermal fluctuations. Our approach is a straightforward exact diagonalization of  $H$ , leading to eigenenergies  $E_n$  associated with eigenstates of the form

$$|n\rangle = \sum_k \sum_{\nu=0}^{N_{\text{ph}}} A_{k, \nu}^{(n)} |k\rangle \otimes |\nu\rangle, \quad (2)$$

where  $|k\rangle$  designates the configurations of two holes with opposite spins distributed over the five cluster sites,  $|\nu\rangle$  de-

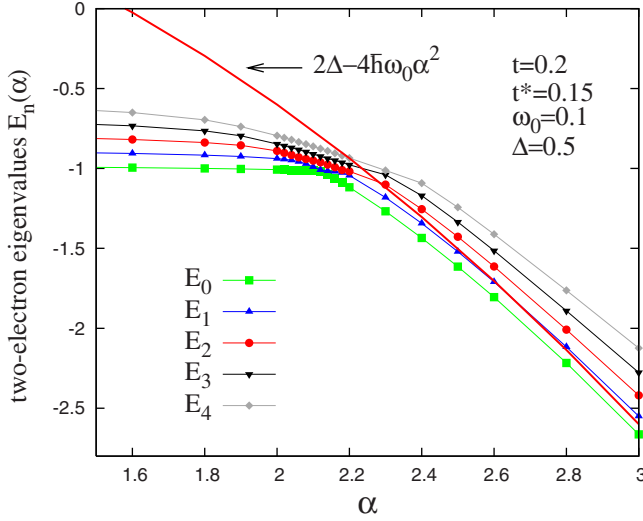


FIG. 3. (Color online) The low-energy two-hole spectrum of  $H$  as a function of the electron-lattice coupling constant  $\alpha$ , showing the crossover between delocalized itinerant states on the plaquette (for  $\alpha \leq \alpha_c = 2.12$ ) and localized bipolaron states on the central polaronic site (for  $\alpha \geq \alpha_c$ ).

notes the  $\nu$ th excited state of the undisplaced harmonic oscillator state, and  $A_{k,\nu}^{(n)}$  is the corresponding weight in the eigenstate  $|n\rangle$ . Taking into account a truncated Hilbert space for the phonon states  $|\nu\rangle$ , we limit ourselves to  $N_{\text{ph}}=70$ . For the set of parameters and temperatures we are concerned with, this is sufficient. We notice from Fig. 3 that the low-energy eigenvalues  $E_n \approx -4t + n\hbar\omega_0$  are relatively unaffected as  $\alpha$  is increased except when they get close to crossing the energy of the localized bipolaron level at some  $\alpha_c$ . As  $\alpha$  is increased above this value, the energy eigenvalues follow the downward trend of the localized bipolaron energy, tending to  $E_n \approx 2\Delta - 4\hbar\omega_0\alpha^2 + n\hbar\omega_0$ .

In Fig. 4 we trace out the occupation probabilities in the two-particle ground state  $|\text{GS}\rangle$  for the configurations with: (i)

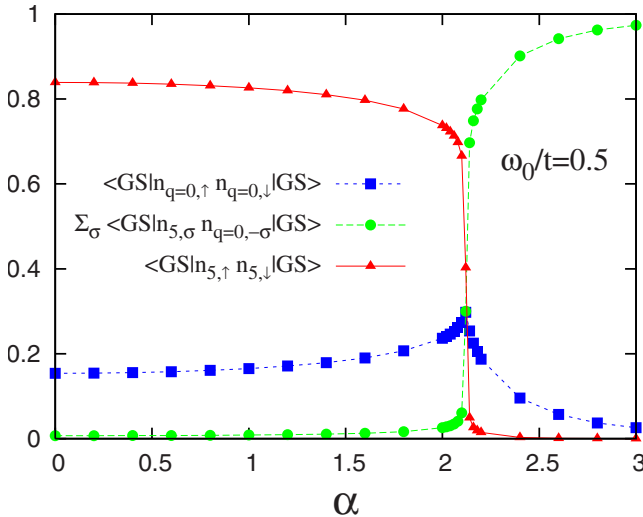


FIG. 4. (Color online) The occupation probabilities for the various possible hole configurations as a function of  $\alpha$  and for  $\omega_0/t = 0.5$ .

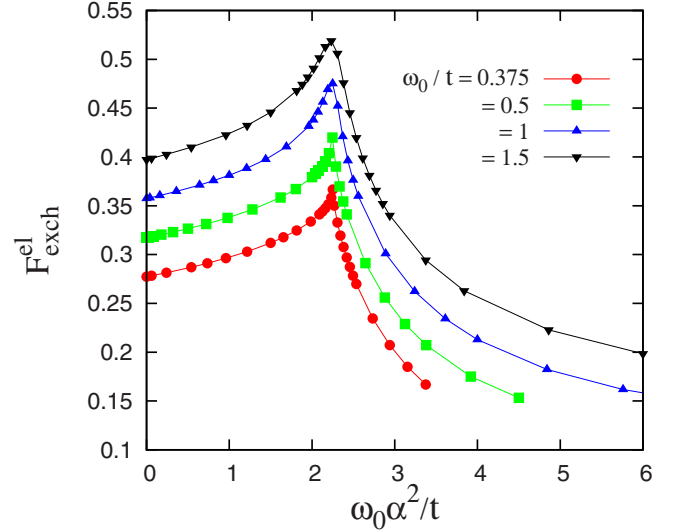


FIG. 5. (Color online) The efficiency factor  $F_{\text{exch}}^{\text{el}}$  as a function of  $\omega_0\alpha^2/t$  for a hole tunneling in and out of a polaronic site, favoring double-charge fluctuations, for several adiabaticity ratios  $\omega_0/t$ . For clarity of presentation, the curves obtained for  $\omega_0/t = 0.5, 1, 1.5$  have been rigidly shifted upward with respect to the one referring to  $\omega_0/t = 0.375$  by amounts equal to 0.04, 0.08, and 0.12, respectively. The numerical values on the y axis thus refer specifically to the case  $\omega_0/t = 0.375$ .

the two holes on the polaronic site,  $\langle \text{GS} | c_{5,\uparrow}^\dagger c_{5,\uparrow} c_{5,\downarrow}^\dagger c_{5,\downarrow} | \text{GS} \rangle$ ; (ii) the two holes on the holes plaquette sites,  $\langle \text{GS} | c_{q=0,\uparrow}^\dagger c_{q=0,\uparrow} c_{q=0,\downarrow}^\dagger c_{q=0,\downarrow} | \text{GS} \rangle$ , where  $c_{q=0,\sigma}^\dagger | 0 \rangle = \frac{1}{2} \sum_{i=1}^4 c_{i,\sigma}^\dagger | 0 \rangle$  signifies the lowest-energy Bloch state of the plaquette; and (iii) the two holes distributed between the two types of sites,  $\sum_{\sigma=\uparrow,\downarrow} \langle \text{GS} | c_{5,\sigma}^\dagger c_{5,\sigma} c_{q=0,-\sigma}^\dagger c_{q=0,-\sigma} | \text{GS} \rangle$ . Figure 4 shows a rapid changeover when we sweep  $\alpha$  through a narrow regime around  $\alpha_c = 2.12$  for  $\omega_0/t = 0.5$ . It is in this narrow regime that we can expect resonant pairing, which means a tunneling of bipolaronic hole pairs from the central site to the plaquette sites and vice versa, in this way inducing a hole pairing on the latter.

The efficiency of double-charge fluctuations is controlled by the ease with which holes tunnel in and out of sites. At zero temperature it is given by the ground-state static correlator

$$F_{\text{exch}}^{\text{el}} = \langle \text{GS} | c_{q=0,\sigma}^\dagger c_{5,\sigma} | \text{GS} \rangle, \quad (3)$$

where  $|\text{GS}\rangle$  denotes the ground state for the two-hole system. The variation of  $F_{\text{exch}}^{\text{el}}$  with  $\alpha$  is illustrated in Fig. 5. We notice that for  $\alpha$  close to zero, the efficiency of such tunneling is governed by the residual tunneling rate determined by the difference in energy between the central site and the lower-lying Bloch states on the plaquette, equal to  $\Delta - 2t$ . As one approaches a certain  $\alpha_c$  from below, we notice a strong increase in this tunneling efficiency. However, when going above  $\alpha_c$ , this efficiency drops rapidly to zero, meaning that the holes are now quasilocalized on the polaronic site in form of bipolarons.

In order to have a double-charge fluctuation-induced superconducting phase, driven by dynamical local lattice instabilities, the above criterion for a high efficiency rate of hole

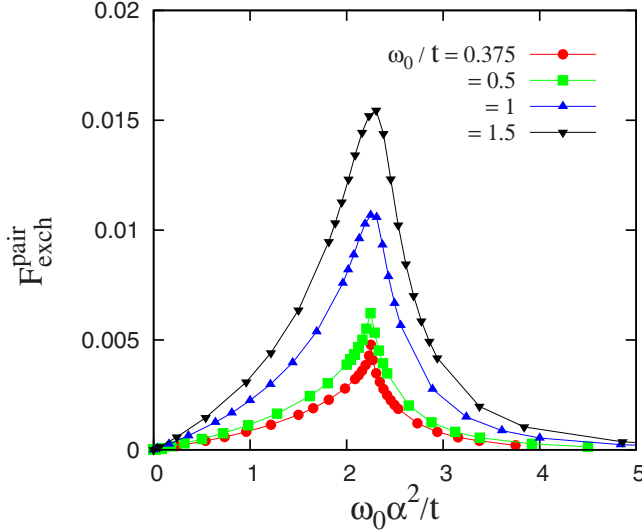


FIG. 6. (Color online) The efficiency factor  $F_{\text{exch}}^{\text{pair}}$  as a function of  $\omega_0 \alpha^2 / t$  for converting, via resonant tunneling, a localized bipolaron on the central polaronic cation-ligand complex into a pair of correlated holes on the ligand environment for several adiabaticity ratios  $\omega_0 / t$ .

tunneling in and out of polaronic sites is not sufficient. What is relevant is the efficiency of coherent double-charge fluctuations between the polaronic site and the plaquette. Such coherent or resonant pair tunneling is given by the efficiency factor

$$F_{\text{exch}}^{\text{pair}} = \langle \text{GS} | c_{5,\uparrow}^\dagger c_{5,\downarrow}^\dagger c_{q=0,\downarrow} c_{q=0,\uparrow} | \text{GS} \rangle - [F_{\text{exch}}^{\text{el}}]^2, \quad (4)$$

where we have subtracted out the rate of exchange of the bipolaron with two holes on the plaquette via incoherent single-hole processes, given by the second term in this expression. The efficiency factor for resonant pair tunneling (see Fig. 6) is sharply peaked near  $\alpha_c$ , its maximal intensity depending on the adiabaticity ratio  $\omega_0 / t$ . The coherent pair tunneling represents only a small fraction of the total tunneling rate, determined largely by its incoherent part. Nevertheless, the size of this coherent component of the two-particle spectral function is sufficient to ensure a high enough condensate fraction in order for a superconducting phase-correlated state to be stabilized. It provides a strong support to the idea that such a mechanism plays a role in real materials which have tendencies to local dynamical lattice instabilities driving double-valence fluctuations.

In order to visualize resonant pair tunneling in and out of the polaronic cation-ligand complex, we examine the evolution with time  $\tau$  of double-charge fluctuations (see Fig. 7). It is described by the correlation function

$$C_{\text{fluct}}^{\text{pair}}(\tau) = \langle \text{GS} | [n_{k=0,\uparrow}(\tau) n_{k=0,\downarrow}(\tau) - n_{5,\uparrow}(\tau) n_{5,\downarrow}(\tau)] \times [n_{k=0,\uparrow}(0) n_{k=0,\downarrow}(0) - n_{5,\uparrow}(0) n_{5,\downarrow}(0)] | \text{GS} \rangle. \quad (5)$$

Near  $\alpha_c = 2.12$  (for  $\omega_0 / t = 0.5$ ), the charge disproportionation follows a smooth oscillation in time with a period  $\omega_0 \tau \approx 70$  and an amplitude varying between  $+0.5$  and  $-0.5$ . When this correlation function is positive and at its maximum, such as for  $\omega_0 \tau = 0, 70, \dots$ , it indicates that both holes are on the cen-

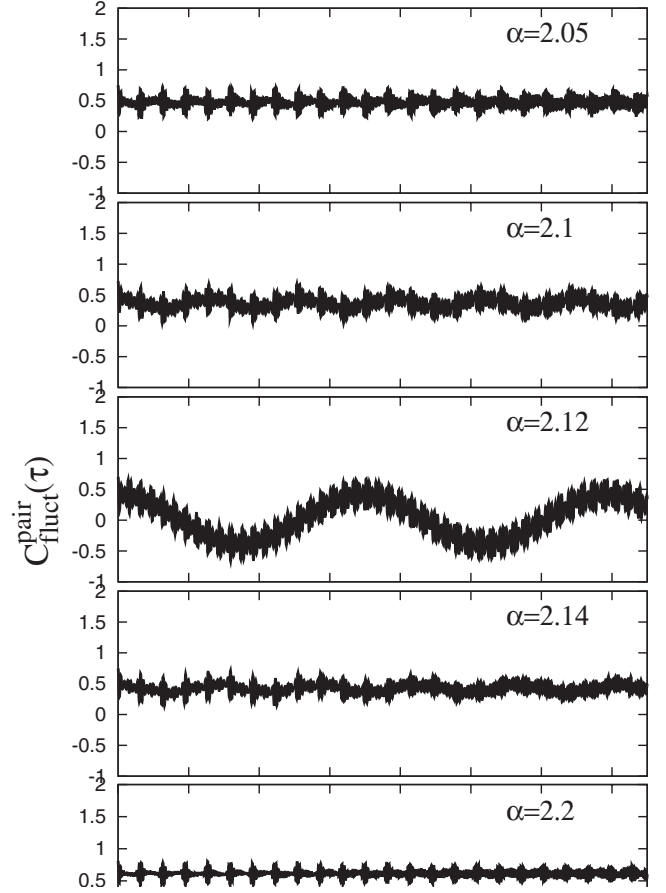


FIG. 7. Evolution in time  $\tau$  of the resonant tunneling of a hole pair in and out of a polaronic site, composed of a cation together with its ligand environment, for  $\omega_0 / t = 0.5$ .

tral polaronic site. If it is negative and maximal, such as for  $\omega_0 \tau = 35, 105, \dots$ , it means that both holes are on the plaquette. The tunneling frequency of the coherent part of this motion of the hole pairs is  $\omega_0^* = (2\pi / \omega_0 \tau) \omega_0 \approx (2\pi / 70) \omega_0 \approx 0.09 \omega_0$ , as we see from Fig. 7. It represents the frequency for a correlated mode, locking together the dynamics of the charge and deformations of the ligand environment or, in our simplified description, of some bond length  $X = \sqrt{\hbar} / 2M \omega_0 [a^\dagger + a]$ . The fluctuations of the latter are described by the correlator

$$C_{\text{fluct}}^{\text{bond}}(\tau) = \langle \text{GS} | [a^\dagger(\tau) + a(\tau)] [a^\dagger(0) + a(0)] | \text{GS} \rangle. \quad (6)$$

Its variation in time  $\tau$  is illustrated in Fig. 8. In line with the fluctuations of the charge distribution, this bond-length fluctuation shows for  $\alpha \approx \alpha_c$  the same smooth oscillating behavior with frequency  $\omega_0^* = 0.09$ , centered around some mean deformation  $\langle \text{GS} | [a^\dagger + a] | \text{GS} \rangle$ . The important feature of such resonant pair tunneling is that the fluctuations, which accompany the systematic motion of the charge distribution as well as of the bond-length,

(i) are on a time scale, typically on the order of  $1 / \omega_0$ , much shorter than the one of the coherent tunneling motion,  $\sim 1 / \omega_0^*$ ; and



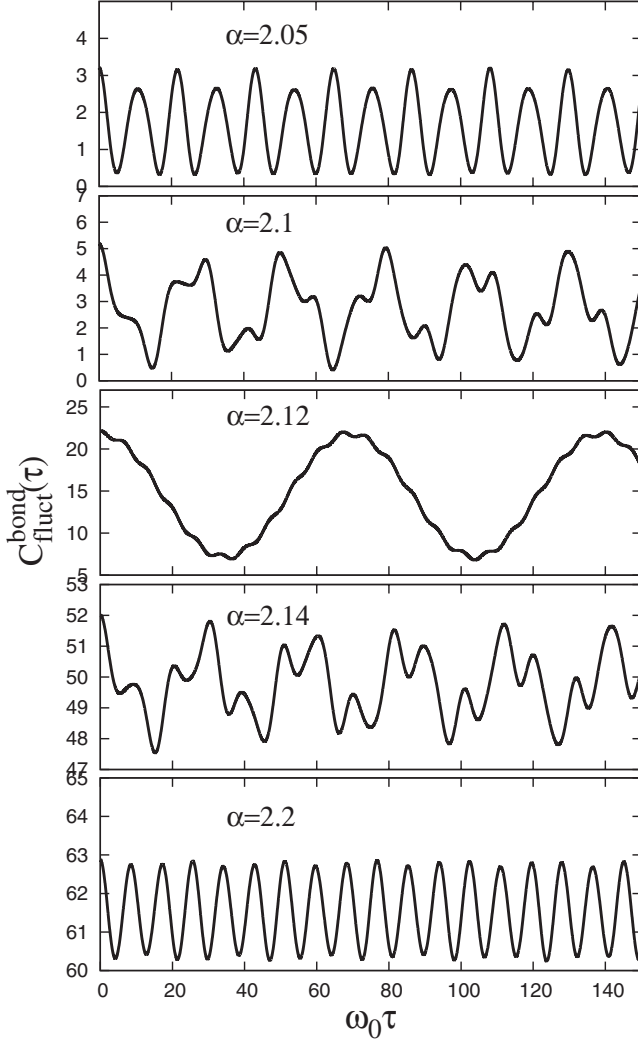


FIG. 8. Evolution in time  $\tau$  of the bond length of the ligand environment which accompanies the resonant tunneling of a hole pair in and out of the cation-ligand complex for  $\omega_0/t=0.5$ .

(ii) have an amplitude which is small compared to the amplitude of the systematic coherent oscillating behavior on the time scale of  $1/\omega_0^*$ .

As soon as we move away from this resonance regime, by tuning  $\alpha$  away from  $\alpha_c$  for a given adiabaticity ratio, the bond-length fluctuations very quickly lose their smooth coherent oscillating behavior. They begin to show phase slips, which, as a result, decorrelate the hole pair fluctuations from those of the bond-length ones. As a result, the hole pairs become *confined* on either the central polaronic site for  $\alpha \geq 2.14$  or the plaquette sites for  $\alpha \leq 2.10$ . In our small system this confinement is inferred from the absence of any sign of periodic motion of the charge and bond-length fluctuations between those two different kinds of sites. This is true for the whole regime of  $\omega_0\tau$  between zero up to at least 20 000. For all intents and purposes, one can therefore regard such a behavior either as a localization for  $\alpha \geq \alpha_c$  of tightly bound hole pairs on the polaronic site or as a confinement for  $\alpha \leq \alpha_c$  of two uncorrelated holes on the plaquette. Incorporating this feature into an infinite lattice structure, such as the one depicted in Fig. 1, we expect that for  $\alpha \geq \alpha_c$  we have a

true charge disproportionation; i.e., the system breaks up into a mixture of cations with localized bipolaronic hole pairs on the cation-ligand sites, leaving the remaining cations without any hole. For the opposite case,  $\alpha \leq \alpha_c$ , we expect a metallic behavior with locally correlated pairing of holes induced by a dynamical charge-exchange coupling with the neighboring polaronic sites. Depending on the overall particle density, this can give rise to: (i) charge-ordered states with translational symmetry breaking, passing from a covalent to ionic bonding;<sup>49</sup> and (ii) correlation-driven insulating states.<sup>35,50</sup>

#### IV. SIGNATURES OF RESONATING BIPOLARONIC DOUBLE-CHARGE FLUCTUATIONS

The phase-correlated dynamics of the charge and the ligand deformation results in several characteristic features in the electronic and lattice properties which are in principle tractable experimentally. Since these features arise from purely local correlations, they are adequately described by the small cluster model system studied here. These features involve:

(i) The strong softening of a local phonon mode with frequency  $\omega_0^R$  (see top panel of Fig. 9), which describes correlated fluctuations of the charge and the local lattice deformations of the cation-ligand complex. This mode is described by the spectral function for bond-length fluctuations, given by

$$B_{\text{ph}}(\omega) = -\frac{1}{\pi} \text{Im} D_{\text{ph}}(\omega), \quad (7)$$

with

$$D_{\text{ph}}(\omega) = \frac{2M\omega_0}{\hbar} \langle\langle X; X \rangle\rangle_{\omega}. \quad (8)$$

At finite temperature  $B_{\text{ph}}(\omega)$  is given by

$$B_{\text{ph}}(\omega) = \frac{1}{Z} \sum_{n,m} e^{-\beta E_m} \langle m | (a^\dagger + a) | n \rangle^2 \delta(\omega + E_n - E_m), \quad (9)$$

with  $Z = \sum_n e^{-\beta E_n}$ . As this local mode softens upon approaching  $\alpha_c$ , its spectral weight  $B_{\text{ph}}(\omega = \omega_0^R)$  strongly increases, reaching a high maximum at  $\omega_0^R(\alpha_c) \equiv \omega_0^*$  (see middle panel of Fig. 9). This is indicative of the large amplitude fluctuations of the bond length, which are necessary to drive the double-charge fluctuations between the polaronic cation-ligand complex and the plaquette sites in a coherent fashion.

(ii) The spectral weight of the zero-frequency bond-length correlation function  $B_{\text{ph}}(\omega=0)$  is practically zero for  $\alpha \leq \alpha_c$ , sharply increases in a narrow region around  $\alpha_c$ , and then continues to grow linearly upon further increasing  $\alpha$  (see bottom panel of Fig. 9). This is indicative of a dynamical local lattice instability, which should manifest itself as a *central peak structure*—a quasielastic peak—in the neutron-scattering cross section. Such features have been observed previously in systems with local dynamical lattice instabilities near ferroelectric phase transitions,<sup>51</sup> martensitic phase transition in A15 compounds,<sup>52</sup> and SrTiO<sub>3</sub>.<sup>53,54</sup>

(iii) The emergence of a double-peak structure in the static pair distribution function (PDF) for the bond length,

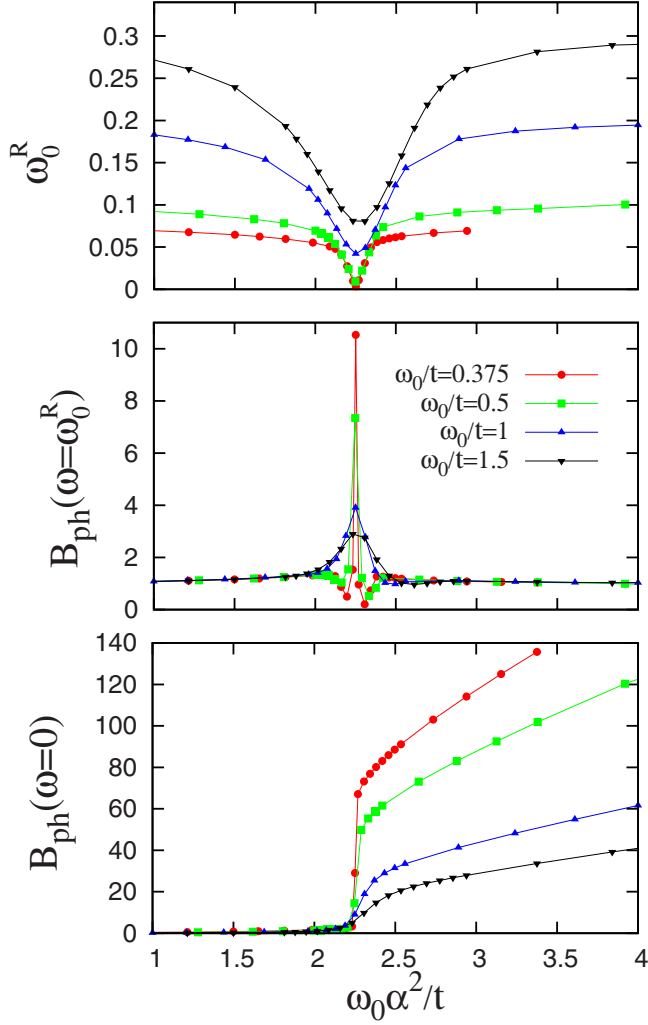


FIG. 9. (Color online) Lattice dynamical signatures related to resonant bipolaronic double-charge fluctuations for several adiabaticity ratios  $\omega_0/t$  and as a function of the electron-lattice coupling  $\omega_0\alpha^2/t$ . The top panel shows the softening of the intrinsic bond-length vibrational mode as one approaches the critical coupling for resonance tunneling at  $\alpha_c \approx \sqrt{(t+\Delta/2)}/\omega_0$ , depending on  $\omega_0/t$ . The maximal softening, occurring for  $\omega_0/t=0.375, 0.5, 1, 1.5$  at  $\alpha_c = 2.45, 2.12, 1.5, 1.22$ , respectively, is given by  $\omega_0^R(\alpha_c)/t \equiv \omega_0^*/t = 0.003\ 36, 0.009\ 07, 0.042\ 05, 0.081\ 03$ . The central panel shows the associated evolution of the spectral weight  $B_{\text{ph}}(\omega=\omega_0^R)$  of this renormalized mode. The bottom panel shows the spectral weight  $B_{\text{ph}}(\omega=0)$  of the zero-frequency mode, related to a static overall shift in the bond length.

$$\begin{aligned}
 g(X) &= \frac{1}{Z} \sum_n e^{-\beta E_n} \langle n | \delta(x-X) | n \rangle \\
 &= \frac{1}{Z} \sum_n e^{-\beta E_n} \sum_k \sum_{\nu, \nu'} A_{k,\nu}^{(n)} A_{k,\nu'}^{(n)} \langle \nu | \delta(x-X) | \nu' \rangle \\
 &\equiv \sum_n \gamma_n(X), \tag{10}
 \end{aligned}$$

which can be measured by neutron spectroscopy or extended x-ray-absorption fine structure (EXAFS). This function has

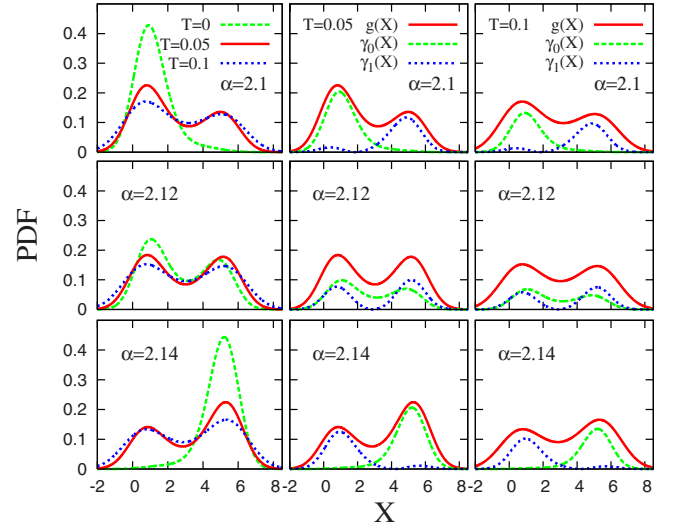


FIG. 10. (Color online) Left panels: pair distribution function  $g(X)$ , measuring the instantaneous distribution of the cation-ligand bond length at the central site, for three values of  $\alpha$  near  $\alpha_c$  and three different temperatures for  $\omega_0/t=0.5$ . Central panels: pair distribution function at  $T=0.05$ , together with the partial contributions  $\gamma_0(X)$  and  $\gamma_1(X)$  coming from the ground state and from the first excited state, respectively. Right panels: same as in the central panels but for  $T=0.1$ .

been investigated in experimental studies concerning the local dynamical lattice topology in the cuprate superconductors and in the manganites for the Cu-O and for the Mn-O bond-stretch modes, respectively. (For a review see the contributions by Sinai *et al.* and by Egami in Ref. 25.)

Our results, shown in Fig. 10, indicate how the PDF evolves near the critical value of  $\alpha_c$ , at which resonant pairing is present, and how it is affected by the temperature. The left column of this figure shows the evolution of the PDF as  $\alpha$  crosses  $\alpha_c$  for several temperatures. At  $T=0$  there is a clear signature for a double-peak structure at  $\alpha_c$ , quickly disappearing as we go away from this resonance condition. At very low temperatures the double-peak-structured PDF can be taken as an indication of resonant pairing. At finite temperature, however, one cannot accredit the double peak to a resonant tunneling of double-charge fluctuations. This becomes clear from the second and third columns of Fig. 10, showing the contributions  $\gamma_0(X)$  and  $\gamma_1(X)$  to the total PDF, coming from the ground state and the first excited state, respectively. At finite temperature, a double-peak structure always arises away from  $\alpha_c$  from thermal excitations, which contribute to the PDF in form of phase-uncorrelated single-peak contributions.

(iv) The onset of strong local pair correlations between the charge carriers below a certain temperature  $T^*$ , resulting in a pseudogap in the local density of states of our cluster. It was in fact on the basis of the present scenario that a pseudogap phase was initially predicted for the cuprates above the superconducting transition.<sup>55,56</sup> Its lattice-driven origin became apparent in the isotope effect experimentally observed<sup>57</sup> on the temperature  $T^*$  at which the pseudogap opens up.<sup>58</sup> Within the same scenario, the onset of the pseudogap feature was found to be related to a change from

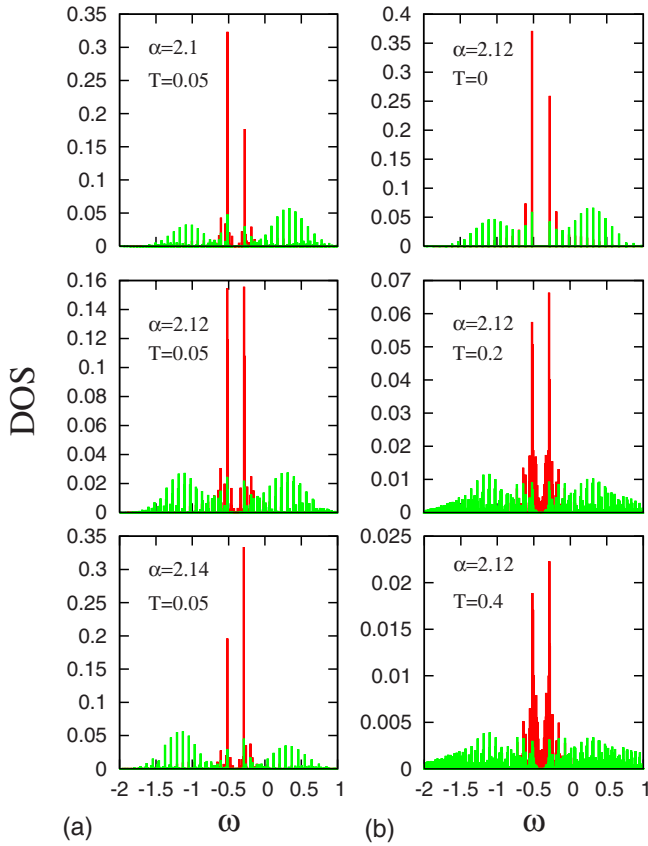


FIG. 11. (Color online) Single-electron DOS decomposed into the contributions coming from the plaquette sites (the spectral lines near the center of the DOS, in red) and from the central polaronic site (the spectral lines at the wings at high frequencies, in green). (a) Evolution of the DOS at low temperature  $T=0.05$  (left column) as  $\alpha$  crosses the critical value for resonant pairing at  $\alpha=\alpha_c=2.12$ . (b) Evolution of the DOS with increasing temperature at  $\alpha_c=2.12$  for  $\omega_0/t=0.5$  (right column), which shows the filling in of the pseudogap with increasing  $T$ . The energy  $\omega$  is in bare units and the pseudogap evolves around  $\Delta - 2\hbar\omega_0\alpha_c^2 \approx -2t = -0.4$ .

single-particle transport at temperature above the onset of the pseudogap ( $T \geq T^*$ ) to one which is controlled primarily by bound charge-carrier pairs below  $T^*$ , upon approaching  $T_c$  from above. These bound pairs then acquire free-particle-like dispersion, which results in a transient Meissner effect<sup>59</sup> (experimentally verified<sup>60</sup>) and remnant Bogoliubov shadow modes in the pseudogap phase.<sup>61</sup> These theoretical results were obtained by assuming an effective local static exchange mechanism between bipolaronic bound hole pairs and itinerant uncorrelated pairs of holes. The present work shows to what extent such a heuristic scenario, investigated within the boson-fermion model, holds true and to what extent a time dependent relaxation of the cation-ligand environment, trapping momentarily the charge carriers in form of bipolarons, permits one to use such an effective double-charge-exchange mechanism.

In Fig. 11 we illustrate separately the contributions to the DOS coming from the holes on the plaquette and those coming from the central polaronic site. The first ones involve the region near the center of the DOS and show a significant amplitude as well as asymmetry. The latter is a consequence

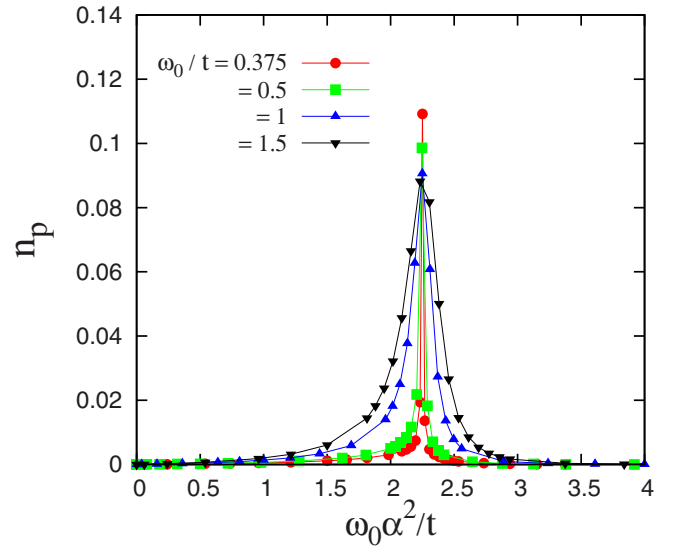


FIG. 12. (Color online) Density  $n_p$  of correlated hole pairs on the plaquette as a function of  $\omega_0\alpha^2/t$ , showing a strong enhancement close to  $\alpha_c \approx \sqrt{(t+\Delta/2)/\omega_0}$  due to resonant pair tunneling. At  $\alpha_c$ ,  $n_p$  is typically on the order of 0.1, which has to be compared with the average total density of holes on the plaquette,  $\sum_{\sigma} \langle \text{GS} | n_{q=0, \uparrow} n_{q=0, \downarrow} \rangle$ , which from Fig. 4 follows to be roughly equal to 0.5.

of the asymmetric charge-lattice deformation coupling which we assumed in this work (see Sec. II). The holes on the polaronic site are responsible for the peaks on either side of the center of the DOS at large frequencies. We notice that as the temperature decreases (right panels of Fig. 11), the pseudogaplike structure turns into a well-defined gap. It is this feature which, on the basis of an effective boson-fermion model treatment,<sup>34,35</sup> finally leads to a true superconducting gap below  $T_c$ .

(v) Resonant pair tunneling in and out of the polaronic cation-ligand complex into the surrounding sites on the plaquette incites pair correlations in the latter. They give rise to the residual pairing in a many-body state, where local diamagnetic fluctuations are embedded in an underlying Fermi sea and eventually result in a macroscopic superconducting phase. Indications of such local diamagnetism in the pseudogap phase of the cuprates have been observed.<sup>62</sup> We illustrate in Fig. 12 the variation with  $\alpha$  (near  $\alpha_c$ ) of the average density  $n_p$ ,

$$n_p = \langle n_{q=0, \uparrow} n_{q=0, \downarrow} \rangle - \langle n_{q=0, \uparrow} \rangle \langle n_{q=0, \downarrow} \rangle, \quad (11)$$

of diamagnetic paired holes on the plaquette and notice that it is quite sizable—about 20% of the total average density of holes on the plaquette at  $\alpha_c$ . Slightly away from this resonant regime, the holes are either pair-uncorrelated (for  $\alpha \leq \alpha_c$ ) or not existent on the plaquette (for  $\alpha \geq \alpha_c$ ), being confined to the polaronic cation-ligand complex as localized bipolarons. The variation with the temperature of  $n_p$  is illustrated in Fig. 13. The contributions to  $n_p$  come primarily from two sources. The first and dominant one comes from the first excited state of the system, lying at an energy  $\omega_0^*$  above the ground state, and reflects the resonant nature of this diamagnetic pairing.

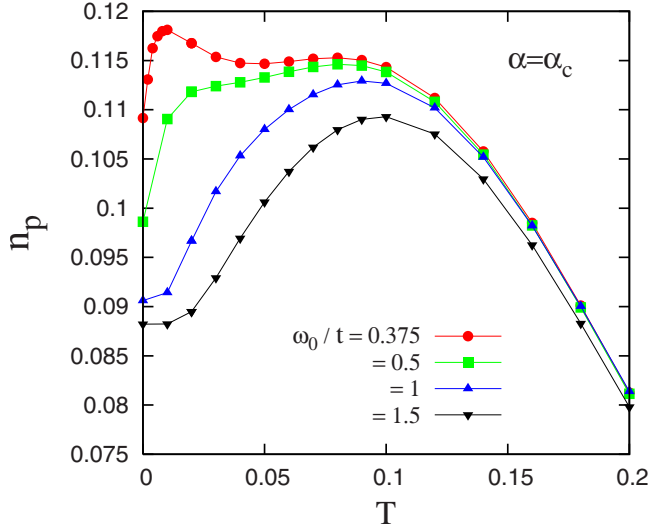


FIG. 13. (Color online) Variation with the temperature  $T$  of the density  $n_p$  of correlated hole pairs on the plaquette for various adiabaticity ratios  $\omega_0/t$  and the corresponding  $\alpha_c$ . With increasing  $T$ ,  $n_p$  rises and then flattens off at some  $T^*$ , which indicates the onset temperature for pair correlations on the plaquettes.

The second contribution comes from the ground state itself, which indicates a static diamagnetic polarization of the holes induced by this resonant pairing effect. As a result, as the temperature increases,  $n_p$  initially increases, then it flattens off at a certain temperature  $T^*$ , and eventually decreases to zero due to thermal fluctuations. We thus take  $T^*$  as a measure of the temperature of the onset of resonant pairing and the opening of the pseudogap of the electronic DOS. The diamagnetism is strongest in the adiabatic regime, where the contribution coming from the resonant pair tunneling is maximal, showing a peak of  $n_p$  at low temperatures. These resonant features are clearly reflected in the dynamical pairing susceptibility (not presented here), which shows a strongly peaked behavior at a frequency  $\omega_0^*$  above the ground-state energy, indicative of the resonant nature of such diamagnetic fluctuations.

## V. SUMMARY

The main objective of the present work was to examine to what extent double-charge fluctuations, driven by local dynamical lattice instabilities, can result in resonant pair tunneling in and out of polaronic cation-ligand complexes, such that spatial phase coherence of these fluctuations on a long-range scale can ultimately be envisaged. This local physics with coherent resonant pair tunneling is a prerequisite for ensuring the existence of *itinerant* bosonic quasiparticles describing diamagnetic local pair fluctuations, embedded in a Fermi sea. It results in the opening of a pseudogap in the single-particle DOS at  $T^*$ , which above  $T_c$  simulates that of a semiconducting phase at finite  $T$ . As  $T$  is decreased, this pseudogap goes over smoothly into the superconducting gap below  $T_c$ , where part of it is still controlled by the gap arising from pair correlations in the normal state.<sup>35</sup> In the strong-coupling antiadiabatic regime, resonant pair tunneling would

reduce to an exclusively bosonic system, composed of localized bipolarons forming static charge disproportionation insulators.<sup>50</sup> Superconductivity in systems with resonant pairing is qualitatively different from that of a BCS state in the sense that its  $T_c$  is controlled by phase rather than amplitude fluctuations, as is the case for the cuprate high- $T_c$  superconductors in the underdoped regime. This requires, on a dynamical basis, a correlated mixture of diamagnetic pairs and quasifree charge carriers, as described by the boson-fermion model in its simplest version, where Hubbard correlation effects, which are certainly important in the cuprates, are neglected.

Using the values of  $\omega_0^*$  and  $n_p$  deduced from the numerical results illustrated in Figs. 9 and 12 and referring to the adiabaticity ratios  $\omega_0/t=0.375, 0.5, 1.0, 1.5$ , we estimate for the superconducting transition temperature the values  $T_c \approx (\xi/a)[4, 10, 20, 27]$  K. Here we have used the approximate expression  $T_c \approx \hbar^2(\xi/a)(n_p/m_p a^2)$  for phase fluctuation-driven superconductivity, where  $\xi$  denotes the coherence length,  $a$  is the lattice constant, and  $n_p$  and  $m_p$  are the number and the mass of the diamagnetic pairs, respectively.  $m_p$  is related to the resonant pair tunneling frequency  $\omega_0^*$  by  $\hbar^2/2m_p = \omega_0^{*2} a^2$ . Within our scenario of a lattice instability-driven superconductivity, such a crude estimate already gives values for  $T_c$  which are quite reasonable. They have been obtained by using a single input parameter,  $\omega_0=50$  meV, taken from experiments concerning the Cu-O bond-stretch mode. It is this mode which shows an anomalous softening for large  $q$  vectors close to the zone boundary and is thought to play an active role in such possible dynamical local lattice instabilities in the cuprate superconductors.<sup>63,64</sup> The value of the electron-phonon coupling  $\alpha$  in this estimate for  $T_c$  is taken at the resonance, i.e.,  $\alpha = \alpha_c = [2.45, 2.12, 1.5, 1.22]$  for the various values of the adiabaticity ratios considered here. The nearest-neighbor and next-nearest-neighbor hopping integrals are taken to be of the same order of magnitude, i.e.,  $t/t^* = 0.2/0.15$ .

We can also estimate the onset temperature  $T^*$  of pairing correlations in the itinerant subsector of the charge carriers. From the behavior of the pairing amplitude  $n_p$ , given in Fig. 13 as a function of the temperature  $T$ ,  $T^*$  should be approximately identified by the crossing point of the tangent to the rising portion of  $n_p$  at low  $T$  and the horizontal line passing through the maximum of  $n_p$ . This  $T^*$  is sensitive to pressure, which increases the local phonon frequency. Using the thermodynamic relation between pressure-induced changes  $\delta T^*$  in  $T^*$  and  $\delta \omega_0^*$  in the local phonon frequency  $\omega_0^*$ ,  $\delta T^*/T^* = \beta(\delta \omega_0^*)/\omega_0^*$  ( $\beta$  denotes a numerical factor of order unity, related to the Grüneisen parameter), this experimentally verified relation<sup>65</sup> for the cuprates with  $\beta \approx -3$  holds for our set of values for  $\omega_0^*$  and  $T^*$  with a  $\beta$  of order unity.

Our concept of resonant pairing-induced diamagnetic fluctuations bears some resemblance to what has been termed Cooper pairing due to overscreening. Overscreening the Coulomb interaction between the electrons implies a negative electronic contribution (besides the positive ionic one) to the static dielectric constant,  $\epsilon_{ei}(\omega=0, q) \leq 0$  for certain  $q=k-k'$  vectors in the Brillouin zone provided that it is smaller than  $-1$ . This overscreening does not result in static global lattice instabilities.<sup>66</sup> It can thus provide a mechanism

for superconducting pairing among holes with wave vectors  $[k, -k']$  for much higher electron-phonon couplings than initially thought. This idea has been brought up again in connections with the cuprate superconductors, where the softening of the Cu-O bond-stretch mode in the Brillouin zone along the directions of the antinodal wave vectors, such as  $[0, \pm 0.5]\pi/a$  and  $[\pm 0.5, 0]\pi/a$ , was interpreted as a signature for overscreening, resulting from local phase-correlated charge and bond-length fluctuations.<sup>67</sup> As we could confirm in the present work, such correlated pair fluctuations do indeed exist and are quite robust. However, based on our study, we do not expect that they give rise to a BCS-type superconducting phase which is controlled by pairing amplitude fluctuations. Such systems should be close to an insulator-to-superconductor transition,<sup>35,36</sup> the insulator being represented by phase-uncorrelated pair fluctuations and the superconductor by spatially phase-correlated ones with a  $T_c$  controlled by phase and not amplitude fluctuations. As far as superconductivity is concerned, our approach to this problem<sup>34-36,56,58</sup> differs from any standard Eliashberg formulation.<sup>63</sup> In the boson-fermion model scenario, superconductivity comes about via a center-of-mass motion of dynamically fluctuating pairs. This is clearly demonstrated by: (i) the early muon-spin-resonance experiments of Uemura *et al.*,<sup>68</sup> showing a  $T_c$  varying with the concentration of superfluid carriers  $n_p$ ; and (ii) a  $T_c \approx 2(\xi/a)[n_p\omega_0^*]$ , which decreases with increasing softening of the bond-stretch mode frequency<sup>69</sup>  $\omega_0 - \omega_0^*$ , where  $\omega_0^*$  determines the inverse mass of these itinerant diamagnetic pair fluctuations. This experimental result<sup>69</sup> relates the doping dependence of  $T_c$  to the local lattice properties, characterized by a softened local mode resulting from dynamical local lattice instability for particular dopings in the superconducting regime.

This tempts us to make the following conjecture for our resonating pair scenario, applied to the superconducting cuprates: Each doping level in these superconducting compounds corresponds to the thermodynamically most unstable single-phase composition in the synthesis. Once stabilized in their solid phase at low temperature, the kinetic stability of those metastable phases is determined by our conditions for resonant pairing. This fixes, for any given bare local mode with frequency  $\omega_0$  (relatively insensitive to doping), a critical charge-ligand deformation coupling  $\alpha_c$ , which will depend on doping and consequently on the degree of softening of this mode.

Resonant pair tunneling poses rather stringent and experimentally verifiable conditions on the local physics, as dis-

cussed here. They are primarily related to features linked to dynamical lattice instability driven by charge fluctuations, such as: (i) the strong softening of a local phonon mode describing the correlated charge-ligand deformation fluctuations (with a frequency  $\omega_0^*$  well below the bare local phonon frequency  $\omega_0$ ); (ii) a quasielastic peak in the neutron-scattering cross section indicative of the dynamical nature of a local lattice instability; (iii) a double-peaked pair distribution function, accessible to neutron-scattering spectroscopy and EXAFS; (iv) locally fluctuating diamagnetism; and (v) a characteristic structure of the electron spectral function, which shows polaronic peaks at large frequencies on either side of the center of the pseudogap and a strongly peaked DOS near this center, coming from the local diamagnetic pair correlations.

The natural next step of the present analysis will have to incorporate these local dynamical features in a large scale system. Here the question arises of the structure of the superconducting state, which will have to involve the phase coherence not only of the charge but also of the lattice instabilities driving the charge pairing. This implies cooperative effects acting between such dynamically fluctuating local clusters, which we expect to result in fluctuating topological structures of the lattice, where insulating correlations compete with superconducting ones.

A field theoretical formulation of the boson-fermion model,<sup>36</sup> not taking explicitly into account the lattice degrees of freedom, has some similarity with the picture of a coarse-grained superconducting state of spatially randomly distributed bosonic modes.<sup>70</sup> However, the main difference between this approach and the one based on the boson-fermion model is that in the latter the local inhomogeneities can fluctuate like in Josephson junction arrays with intergrain tunneling.

Treating the cuprates within this scenario will require as a next step a microscopic treatment of the ligand environment. This means: (i) explicitly taking into account the different formal valence states of the Cu-ligand complex; (ii) incorporating the strong Hubbard  $U$  correlations in our present scheme, resulting in local Zhang-Rice singlets; and (iii) studying the dynamical charge exchange between such cation-ligand complexes and the surrounding metallic matrix beyond the single cluster model (discussed here) and beyond any adiabatic approximation.<sup>71</sup> These and other related questions will be dealt with in some future work.

<sup>1</sup>J. M. Vandenberg and B. T. Matthias, *Science* **198**, 194 (1977).

<sup>2</sup>C. S. Ting, D. N. Talwar, and K. L. Ngai, *Phys. Rev. Lett.* **45**, 1213 (1980).

<sup>3</sup>J. E. Hirsch and D. J. Scalapino, *Phys. Rev. B* **32**, 5639 (1985).

<sup>4</sup>H.-B. Schüttler, M. Jarrell, and D. J. Scalapino, *Phys. Rev. B* **39**, 6501 (1989).

<sup>5</sup>A. Taraphder and P. Coleman, *Phys. Rev. Lett.* **66**, 2814 (1991).

<sup>6</sup>M. B. Robin and P. Day, *Adv. Inorg. Chem. Radiochem.* **10**, 247 (1967).

<sup>7</sup>I. A. Chernik and S. N. Lykov, *Fiz. Tverd. Tela (Leningrad)* **23**, 2956 (1981) [*Sov. Phys. Solid State* **23**, 1724 (1981)].

<sup>8</sup>B. Ya. Moizhes and I. A. Drabkin, *Fiz. Tverd. Tela (Leningrad)* **25**, 1974 (1983) [*Sov. Phys. Solid State* **25**, 1139 (1983)].

<sup>9</sup>C. M. Varma, *Phys. Rev. Lett.* **61**, 2713 (1988).

<sup>10</sup>Y. Matsushita, H. Bluhm, T. H. Geballe, and I. R. Fisher, *Phys. Rev. Lett.* **94**, 157002 (2005).

<sup>11</sup>C. K. Jørgensen and L. Jansen, *Sov. Phys. Solid State* **63**, 1325 (1989).

- <sup>12</sup>I. Hase and T. Yanagisawa, Phys. Rev. B **76**, 174103 (2007).
- <sup>13</sup>Y. I. Ravitch, in *Lead Chalcogenides: Physics and Applications*, edited by D. Khokhlov (Taylor & Francis, New York, 2003).
- <sup>14</sup>W. A. Harrison, Phys. Rev. B **74**, 245128 (2006).
- <sup>15</sup>P. W. Anderson, Phys. Rev. Lett. **34**, 953 (1975).
- <sup>16</sup>H. Feshbach, Ann. Phys. (N.Y.) **5**, 357 (1958).
- <sup>17</sup>A. W. Sleight, J. L. Gillson, and P. E. Bierstedt, Solid State Commun. **17**, 27 (1975).
- <sup>18</sup>A. Simon, Chem. Unserer Zeit **22**, 1 (1988).
- <sup>19</sup>S. Lakkis, C. Schlenker, B. K. Chakraverty, R. Buder, and M. Marezio, Phys. Rev. B **14**, 1429 (1976).
- <sup>20</sup>B. K. Chakraverty, M. J. Sienko, and J. Bonnerot, Phys. Rev. B **17**, 3781 (1978).
- <sup>21</sup>O. F. Schirmer and E. Salje, J. Phys. C **13**, L1067 (1980).
- <sup>22</sup>J. A. Wilson, J. Phys. C **20**, L911 (1987).
- <sup>23</sup>J. Lee, K. Fujita, K. McElroy, J. A. Slezak, M. Wang, Y. Aiura, H. Bando, M. Ishikado, T. Masui, J.-X. Zhu, A. V. Balatsky, H. Eisaki, S. Uchida, and J. C. Davis, Nature (London) **442**, 546 (2006).
- <sup>24</sup>J. Ranninger and A. Romano, Europhys. Lett. **75**, 461 (2006).
- <sup>25</sup>See, for instance, *Polarons in Bulk Materials and Systems of Reduced Dimensionality*, edited by G. Iadonisi, J. Ranninger, and G. De Filippis (IOS, Amsterdam, 2006).
- <sup>26</sup>P. Benedetti and R. Zeyher, Phys. Rev. B **58**, 14320 (1998).
- <sup>27</sup>D. Meyer, A. C. Hewson, and R. Bulla, Phys. Rev. Lett. **89**, 196401 (2002).
- <sup>28</sup>M. Capone and S. Ciuchi, Phys. Rev. Lett. **91**, 186405 (2003).
- <sup>29</sup>M. Hohenadler, M. Aichhorn, and W. von der Linden, Phys. Rev. B **68**, 184304 (2003).
- <sup>30</sup>M. Hohenadler, D. Neuber, W. von der Linden, G. Wellein, J. Loos, and H. Fehske, Phys. Rev. B **71**, 245111 (2005).
- <sup>31</sup>P. Quémerais, Mod. Phys. Lett. B **9**, 1665 (1995).
- <sup>32</sup>G. Rastelli, S. Fratini, and P. Quémerais, Eur. Phys. J. B **42**, 305 (2004).
- <sup>33</sup>Ph. Phillips and D. Dalidovich, Science **302**, 243 (2003).
- <sup>34</sup>T. Stauber and J. Ranninger, Phys. Rev. Lett. **99**, 045301 (2007).
- <sup>35</sup>M. Cuoco and J. Ranninger, Phys. Rev. B **74**, 094511 (2006).
- <sup>36</sup>M. Cuoco and J. Ranninger, Phys. Rev. B **70**, 104509 (2004).
- <sup>37</sup>E. Altman and A. Auerbach, Phys. Rev. B **65**, 104508 (2002).
- <sup>38</sup>P. W. Anderson, Science **235**, 1196 (1987).
- <sup>39</sup>M. Capone, P. Carta, and S. Ciuchi, Phys. Rev. B **74**, 045106 (2006).
- <sup>40</sup>A. C. Hewson and D. Meyer, J. Phys.: Condens. Matter **14**, 427 (2002).
- <sup>41</sup>W. Koller, D. Meyer, and A. C. Hewson, Phys. Rev. B **70**, 155103 (2004).
- <sup>42</sup>J. E. Hirsch, Phys. Rev. Lett. **59**, 228 (1987).
- <sup>43</sup>F. C. Zhang and T. M. Rice, Phys. Rev. B **37**, 3759 (1988).
- <sup>44</sup>J. Röhlér, Int. J. Mod. Phys. B **19**, 255 (2005).
- <sup>45</sup>B. H. Toby, T. Egami, J. D. Jorgensen, and M. A. Subramanian, Phys. Rev. Lett. **64**, 2414 (1990).
- <sup>46</sup>A. W. Sleight, Phys. Today **44**(6), 24 (1991).
- <sup>47</sup>J. Röhlér (private communication).
- <sup>48</sup>C. J. Morningstar and M. Weinstein, Phys. Rev. D **54**, 4131 (1996).
- <sup>49</sup>J. B. Goodenough and J.-S. Zhou, Phys. Rev. B **49**, 4251 (1994).
- <sup>50</sup>J.-M. Robin, A. Romano, and J. Ranninger, Phys. Rev. Lett. **81**, 2755 (1998).
- <sup>51</sup>W. Cochran, Adv. Phys. **9**, 387 (1960).
- <sup>52</sup>G. Shirane and J. D. Axe, Phys. Rev. Lett. **27**, 1803 (1971).
- <sup>53</sup>G. J. Coombs and R. A. Cowley, J. Phys. C **6**, 121 (1973).
- <sup>54</sup>T. Riste, E. J. Samuelson, K. Otnes, and J. Feder, Solid State Commun. **9**, 1455 (1971).
- <sup>55</sup>J. Ranninger, R. Micnas, and S. Robaszkiewicz, Ann. Phys. (Paris) **13**, 455 (1988).
- <sup>56</sup>J. Ranninger, J. M. Robin, and M. Eschrig, Phys. Rev. Lett. **74**, 4027 (1995).
- <sup>57</sup>D. Rubio Temprano, J. Mesot, S. Janssen, A. Furrer, K. Conder, and H. Mutka, Phys. Rev. Lett. **84**, 1990 (2000).
- <sup>58</sup>J. Ranninger and A. Romano, Phys. Rev. B **71**, 184520 (2005).
- <sup>59</sup>P. Devillard and J. Ranninger, Phys. Rev. Lett. **84**, 5200 (2000).
- <sup>60</sup>J. Corson, R. Mallozzi, J. Orenstein, J. N. Eckstein, and I. Bozovic, Nature (London) **398**, 221 (1999).
- <sup>61</sup>T. Domanski and J. Ranninger, Phys. Rev. Lett. **91**, 255301 (2003).
- <sup>62</sup>Y. Wang, L. Li, M. J. Naughton, G. D. Gu, S. Uchida, and N. P. Ong, Phys. Rev. Lett. **95**, 247002 (2005).
- <sup>63</sup>M. Tachiki, M. Machida, and T. Egami, Phys. Rev. B **67**, 174506 (2003).
- <sup>64</sup>D. Reznik, L. Pintschovius, M. Ito, S. Iikubo, M. Sato, H. Goka, M. Fujita, K. Yamada, G. D. Gu, and J. M. Tranquada, Nature (London) **440**, 1170 (2006).
- <sup>65</sup>P. S. Häfliger, A. Podlesnyak, K. Conder, and A. Furrer, Europhys. Lett. **73**, 260 (2006).
- <sup>66</sup>D. A. Kirzhnits, Usp. Fiz. Nauk **119**, 357 (1976) [Sov. Phys. Usp. **19**, 530 (1976)]; *Problema Vysokotemperaturnoi Sverkhprovodimosti*, edited by V. L. Ginzburg and D. A. Kirzhnits (Nauka, Moscow, 1977); *High-Temperature Superconductivity* (Consultants Bureau, New York, 1982).
- <sup>67</sup>M. Tachiki and S. Takahashi, Phys. Rev. B **38**, 218 (1988).
- <sup>68</sup>Y. J. Uemura, G. M. Luke, B. J. Sternlieb, J. H. Brewer, J. F. Carolan, W. N. Hardy, R. Kadono, J. R. Kempton, R. F. Kiefl, S. R. Kreitzman, P. Mulhern, T. M. Riseman, D. L. Williams, B. X. Yang, S. Uchida, H. Takagi, J. Gopalakrishnan, A. W. Sleight, M. A. Subramanian, C. L. Chien, M. Z. Cieplak, Gang Xiao, V. Y. Lee, B. W. Statt, C. E. Stronach, W. J. Kossler, and X. H. Yu, Phys. Rev. Lett. **62**, 2317 (1989).
- <sup>69</sup>T. Egami, Physica C **460-462**, 267 (2007).
- <sup>70</sup>A. V. Balatsky and J.-X. Zhu, Phys. Rev. B **74**, 094517 (2006).
- <sup>71</sup>L. Hozoi and S. Nishimoto, Phys. Rev. B **73**, 245101 (2006).